Published by :
http://www.ijert.org

International Journal of Engineering Research & Technology (IJERT)
ISSN: 2278-0181
Vol. 8 Issue 07, July-2019

CFD Simulation of Fluid Flow and Heat Transfer in Micro Channels

Shivaji Rao Devakathe
M. Tech. Student, Mechanical Engg.
Narsimhareddy Engineering College
Hyderabad, India

Rajesh S.
Assistant Professor, Mechanical Engg.
Narsimhareddy Engineering College
Hyderabad, India

Satish Kumar G.
Associate Professor, Mechanical Engg.
Narsimhareddy Engineering College
Hyderabad, India

***Abstract*—Numerical simulation of fluid flow & heat transfer was performed for a Parallel micro-channel array. Generalized transport equations are discretized & solved in three dimensions to find out the pressure, temperature & velocities. The Reynolds number ranges from 50 to 400 were used and aspect ratios range from 0.10 to 1.0 used in the present study. For simulates thermal energy generation from an integrated circuit a constant heat flux of 90 W/cm^2 is applied to the northern face of the computational domain. In this study it was observed that the apparent friction coefficients linearly increase with Reynolds number, which is explained by increased entry length for higher Reynolds number flows. In the microchannels the mean temperature of water also increases with channel length after the short thermal entry region. With increasing Reynolds number and aspect ratio inlet & outlet thermal resistance value decrease for large aspect ratios (i.e., 0.75 and 1). Thermal & friction coefficient results do not differ significantly for large aspect ratios, but results for small aspect ratios (i.e., 0.1 and 0.25) notably differ from results of other aspect ratios.**

Keywords—Microchannel; Heat Transfer; Fluid Flow; Numerical Simulation

I. INTRODUCTION

Over a few years ago, micro-channels are used as a potential solution for dissipating the thermal energy from densely packed integrated circuit board. There are many proposals and researches has been mad which are indicating that high rate of heat fluxes could be dissipated by using a fluid passage through the micro-channels, which offers the increased ratio of surface area to volume of the channel. Micro-channels can also be placed directly on the integrated circuit substrate. The advantage of this placing on the substrate is to reduce the heat resistance from heat source (integrated circuit board) to heat sink (i.e to atmosphere). To avoid any disturbance of circuit function, the microchannels can be inbuilt or modeled onto or etched into the electrically on the inactive side of the chip of the circuit. The work of previously modeled microchannel pioneers initiated many research and development of microchannels, further development of the other micro-fluid devices including ink jet printers, heat exchangers, chemical reactors, fuel cells, micro-pumps, and biomedical devices to increase the dissipation rate of heat[1-5].

Many of the investigators bring up the differences between micro-scale and macro-scale fluid flow and heat transfer. While the other investigators has done these on basing the similarities between the flow regimes. beginning the research, it is necessary to understand the scale on which the flow and thermal physics always occurring. among other researchers, Bontemps [[6] explained the usefulness of Knudsen number(Kn) as it is a valid indication of the continuum for the flow of the fluid in a channel of the specified length scale. The Knudsen number is the ratio of the molecular mean free path to the channel characteristic length. Mala and Li [7-9]reported that the increment in the friction factors are been predicted from a reduction in Navier Stokes, and the difference become more and more with decrement of the microtube diameter. These effects are been attributed to an early transition flow to turbulent flow. While changing surface roughness of the tube it effects are determined by testing the tubes of various materials . Wu and Cheng [10-11] named two investigators measured the friction factor and Nusselt number for laminar water flow in microchannels of trapezoidal cross sections. He investigated the channel geometries were varied, Surface roughnesses, surface hydrophilic properties, correlations were presented for Nusselt number and friction factor as functions of these variables. The surfaces which are with the usage of different hydrophilic properties were silicon and bare silicon with a wave length range of 5000Å with thermal oxide coating. Bontemps has recently published a figure that shows ($Nu_{exp}/Nu_{classical}$) and($f_{exp}/f_{classical}$) is the function of published paper starting from the year 1990 to 2004 [12-16]. The plot which is used of these ratios have shown a clear convergence towards a value of one as the years has been approaching 2004 [17-21]. Although this is not published in other sources, Bontemps extrapolates the results that the classical (Navier Stokes and energy equations) theories can be made applicable on thelevel of the micro .

This research work has been made to aspire at a better understanding of thermal and hydraulic performance of water in a parallel series placement of rectangular microchannels. the finite volume technique is used to solve the 3-dimensional flow and energy equations in both the solids and regions. The research objectives of the present study are:

1. To create a numerical code that can be used to create simulations of 3-dimensional temperature, pressure and velocity distributions in a parallel layout of the rectangular microchannels.
2. To numerically carry out these thermally repeated boundary conditions for the repeating series of microchannels.
3. By comparing thermal resistance and apparent friction coefficient which is received from the numerical simulation is to be taken from experimental data.

International Journal of Engineering Research & Technology (IJERT)
ISSN: 2278-0181
Vol. 8 Issue 07, July-2019

4. To present these results of the numerical simulation in the form of friction coefficient requires pumping pressure vs. flow rate, thermal resistance, and maximum substrate temperature for the Reynolds number varies from 50 to 400 and aspect ratio is also varies from 0.1 to 1.0.

5. By the analysis of effects of the viscous distribution on the replacement of bulk temperature for any one of the case of aspect ratio.

II. Model Formulation

Numerical models can be made based upon the overlying theory or assumptions. While these results of the made model is always the dependent upon the many factors during the development of model, these results can't provide more insights so that the physical phenomena that given by these governed equations and assumptions. Numerical codes have to be often developed because that the governing equations are always difficult to solve, tightly coupled, nonlinear, or because data used as input to the equations are discrete.

The various cases which are considered in this research work is the single-phase forced and convective flow of the water in the array of parallel and microchannels through it. Convective heat transfer is a transfer of thermal energy is used in the presence of a temperature difference with the combination of bulk fluid motion (advection) and random molecular motion (diffusion). Since the provided liquid water has been always used to force them through channels by means on the external pump provided for it,mode of liquid and heat transfer is known as the forced convective transfer. Velocity components which appear in these convective terms of energy equation, so this solution for the energy equation is depending upon the converged solution for the flow field.

The density of water which does not change appreciably with the increase of temperature,and as a result, mixed convection (free and forced convection) effects are not been considered in it. If gas flows were also considered in this study, the mixed convection is used in addition to the slip boundary conditions for the velocity would likely to be included. Since the objectives of these studies is to compare the numerical results with that of experimental data, geometry and the experimental conditions to be described, and subsequent discussions will be focusing on that equations and boundary conditions that can also be used to model thermo hydraulic behavior of the liquid water in a microchannel array

A. Description of Test Case

The cross section is considered as 100ìm wide which is also the same value as pitch is the repeated array, and all microchannels are about 10mm long. For thermal analysis, any repeated cross sectional geometry could also to be modeled because of this thermally repeated boundary condition may also be applied in the z-direction.

This means that these channels could be centered in cross section shown in Fig 1,and that the thermal model would be given similar results for the temperature distributions with in fluid and solid regions.

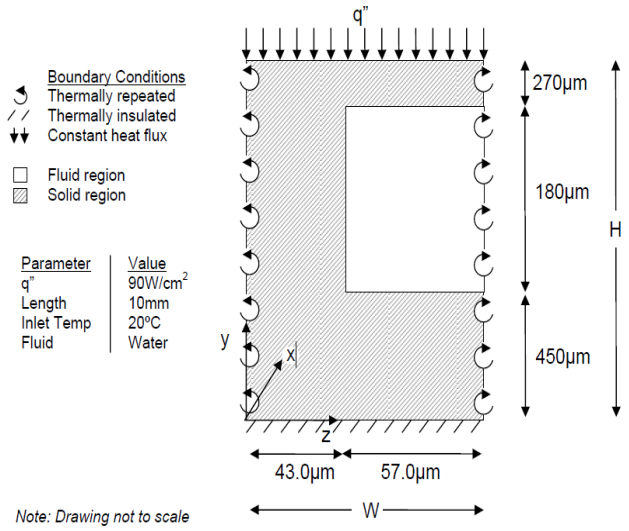

Fig. 1. Y-Z cross section and boundary conditions for the rectangular microchannel

The case shown in the Fig 1 has the hydraulic diameter of 86.58ìm. Additional geometries are to be numerically modeled which have been the same hydraulic diameter and vertical centering, *C* but they all have different aspect ratios as shown in the Fig 2. Dimensions are for each of geometries shown in Fig 2 are also given in Table I. Each of these geometries shown in Fig 2 will has the thermally repeated boundary conditions applied in the z-direction.

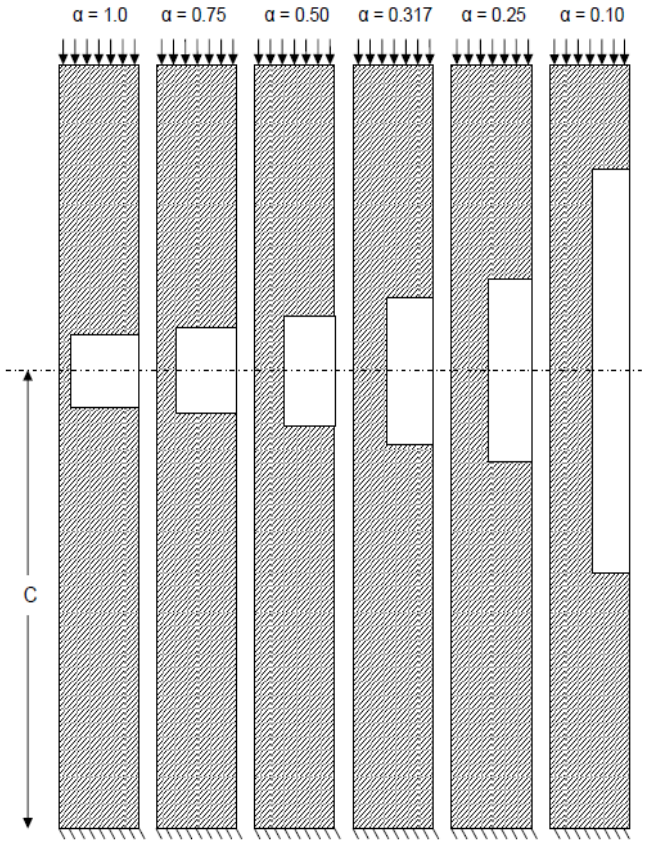

Fig. 2. Aspect Ratio and scale geometries of the six rectangular channels considered

International Journal of Engineering Research & Technology (IJERT)
ISSN: 2278-0181
Vol. 8 Issue 07, July-2019

TABLE I. DIMENSIONS OF CHANNEL GEOMETRIES FOR CASES OF DIFFERENT ASPECT RATIO

Aspect Ratio α (w/h)	Channel Height, h (μm)	Channel Width, w_c (μm)	Domain Height, H (μm)	Domain Width, W (μm)	Center Height, C (μm)
0.10	476.2	47.62	900.	100.	431.78
0.25	216.5	54.11	900.	100.	431.78
0.317	180.0	57.00	900.	100.	431.78
0.50	129.9	64.94	900.	100.	431.78
0.75	101.0	75.76	900.	100.	431.78
1.0	86.58	86.58	900.	100.	431.78
The channel length and domain length are 10mm for all cases of aspect ratio.					

B. Basic Equation and Boundary Conditions

This may be considered to be laminar forced convection of the water, a Newtonian fluid, in an array of the silicon micro channels. As shown in the Section 2, the dimensions of these problems allow the standard continuum hypothesis which has to be applied while modeling behavior of the water flow in the channels .

The following are the assumptions made for the numerical model :

1. Laminar flow
2. Steady state flow and heat transfer
3. Water is incompressible
4. Gravitational forces are also negligible
5. Radiation heat transfer is as negligible as compared to the convection to diffusion heat transfer
6. Buoyancy forces are also negligible
7. Internal heat-generation is not present aside from the viscous heating
8. It will have constant solid properties
9. The fluid properties are the dependent on the average of the outlet and inlet temperatures only, which are a function of the Reynolds number when the heat flux is constant.

Simulation of the fluid flow and heat transfer in the section of the repeated geometry will also require the solutions for the non-linear and 3-dimensional. The Navier Stokes equation and the solution for the conjugate (solid and fluid) energy equation. Shah and London indicating that the entry length in the problem can be solved either by linearizing the momentum and equation or also by using a finite difference and method. Although the more rapidly the developing flow is the modeled by the linearization method,the corrections can also be applied to the counteract this problem. This method is also providing a solution for the fluid flow in the three dimensional channel, but these velocities in the above transverse directions are neglected. This study uses the finite volume method, because it always provides the better solution for these conjugate heat transfer problem, even all velocity components are considered, and the finite volume method is always known to give the accurate results without there is a necessity of adding the corrections to model. The finite volume method must also is to be use the flow and energy equations in the three dimensions is as a starting point. The flow of the equations are the nonlinear and conjugate nature of the energy problems difficulty is also to the energy equation. In the such a case of nonlinear and the conjugate problem, no closed form solution may also be obtained for also the temperature, pressure, and all the three velocity components are simultaneously, so for an appropriate the numerical scheme must also be provided. Work uses finite-volume technique described by the Patankar because of the computational accuracy and the ease of implementation. This method is also reffed as the control volume formulation.

C. GRID INDEPENDENCE

Three different grid sizes and a non uniform grid size were used In the grid independence study. control volumes in the solid region were larger than those in the fluid region because the velocity of solid region is zero and the Thermal conductivity is very high as compared to the fluid, The grid independence study results are tabulated in Table II, below. According to the results, very low percentage of differences between cases are obtained. Therefore, the case is declared as grid independent .

TABLE II. GIRD INDEPENDENCE STUDY PARAMETERS

Case	Number of Elements	Number of Nodes	$f_{app}Re$	$R_{t,Outlet}$
1	124850	151200	85.27	$7.232x10^{-2}$
2	28180	951468	86.24	$7.237x10^{-2}$
3	977120	1223215	86.67	$7.231x10^{-2}$

The values of x, y, and z are given in Table III. The values of pressure gradient, velocity, and temperature gradient are constant after the entry region hence coarser grid is used. Furthermore, the velocities are zero within the solid region and temperature gradients are small compared to those in the fluid region there a coarser grid is also used. To Obtain accurate velocity and temperature gradients Each solid control volume bordering the fluid region was given the same size as those in the fluid region.

TABLE III. MESH PARAMETERS

Sl No	Mesh Parameters	
1	Size function	Proximity
2	Relevance Center	Fine
3	Initial Size seed	Active assembly
4	Transition	Slow
5	Span angle center	Fine
6	Number of cells across G..	Default (3)
7	Proximity Size function	Faces and Edges
8	Proximity Min Size	$1.039_{e\text{-}0.002}$ mm
9	Max Face Size	$1.039_{e\text{-}0.002}$ mm
10	Max Tet Size	$1.039_{e\text{-}0.002}$ mm
11	Growth Rate	Default (1.20)

International Journal of Engineering Research & Technology (IJERT)
ISSN: 2278-0181
Vol. 8 Issue 07, July-2019

III. Results and Discussion

By solving Finite Volume Method *u*, *v*, and *w* temperature field, velocity fields and pressure field in 3 dimensions were obtained. This Method was used to solve these fields for each of the geometries shown in Fig 2 as Reynolds number was varies from 50 to 400. once the converged temperature, pressure and velocity fields were obtained, Other values such as friction coefficient, mean temperature and thermal resistance were calculated .

A. Comparison with experimental data

one of the objectives of this work is to compare the values obtained from computational results such as apparent thermal resistance and friction coefficient with available experimental data [3]. The geometry used to gather experimental data, and the numerical computations used this same geometry is shown in Fig 1. The Equations for apparent friction coefficient and outlet thermal resistance. Eq. (1) gives equation for inlet thermal resistance, where $T_{w,inlet}$ is defined as the temperature of substrate at y = H at the channel inlet

$$R_{t,inlet} = \frac{T_{w,inlet} - T_{f,inlet}}{q''} \qquad \text{ϰ+ς}$$

Due to entry effects Local convection coefficients are larger at the channel inlet than at the channel outlet, and the inlet thermal resistance. when more thermal energy is transferred to the fluid near the channel entrance the substrate temperature near the channel entrance will decrease and the thermal resistance will be lower. If less amount of thermal energy is transferred, which will increase the temperature of substrate near the channel entrance and the convection coefficient will be lower,and consequently the thermal resistance will be higher. The comparison of apparent friction coefficient values between the present numerical study and the experimental work of Kawano et al. [3] is shown in Figure 6.1. When experimental uncertainty is considered It shows good agreement between the experimental r esults and the present numerical computation. The uncertainty range varies between 12% and 15%. the variation of apparent friction coefficient is linear In the range of Reynolds number .This result differs from the fully developed friction factor results which are widely used as a basis of comparison for laminar flows in microchannels. For the geometry considered, the fully developed flow friction coefficient is 69.2 [26], which does not match the data for Reynolds number beyond 250.

increased hydrodynamic entry length causes proportional increase of apparent friction coefficient with increasing Reynolds number. In the entry region, which the flow is not developed causes large velocity gradients thus lead to increased pressure drop. When the entry region increases in length with increasing Reynolds number, a higher pressure drop will be evident within the channel. In the laminar region for all Reynolds numbers the local friction coefficient values are equal to the fully developed flow friction coefficient values. For the same boundary conditions and geometry The present numerical results are nearly same as the numerical results of [20] and [21]. Many experimental investigations of microchannels cite early transition to turbulence because of increasing friction coefficient with increasing Reynolds number. If we take the case of Reynolds number into consideration The entrance length can be on the order of 10-20% of the channel length [26]. Within the laminar region For higher Reynolds numbers The entrance region may extend beyond the channel length. The extension of the entrance region causes much higher friction coefficients than those predicted by fully-developed laminar flow correlations

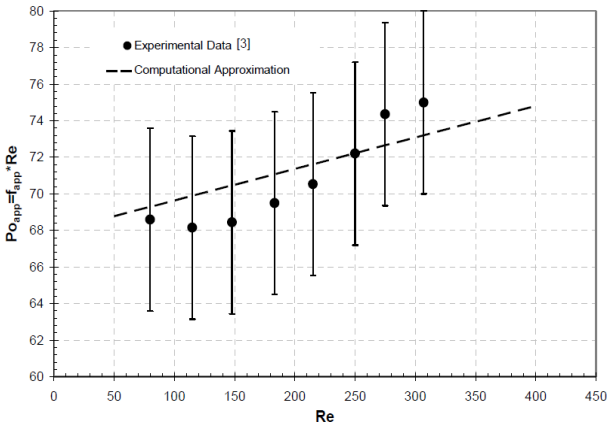

Fig. 3. Comparison of present computational results of apparent friction coefficient with the experimental data of Kawano et al. [3]

B. Numerical Results for all Geometries

As previously discussed ,the velocity profile is uniform at the entrance, and it takes a finite length for the velocity profile to become fully developed (independent of length) . The developing velocity profiles at the channel midlines for both the y- and z-cross sections for a Reynolds number of 400 and aspect ratio of 0.10 were shown in Figure 6.3. In the y-direction The velocity profile appears flat for fully developed flow because the channel is ten times longer in the y-direction than in the z-direction. Thus, the narrow z-direction largely influences velocity profile.From Figure 6.3 we can observe that the flow is hydrodynamically fully developed at approximately 11% of the channel length, or 1.1mm.The solid region is shown in these figures to emphasize the fact that the solid region was included in the computational domain and to provide the reader with a sense of scale.

In Fig 3, the apparent friction coefficient was compared with experimental data for an aspect ratio of 0.317, the apparent friction coefficients for all aspect ratios considered in this study are given in Fig 4. As in the case for 0.317 aspect ratio all other aspect ratios have the same general trend of T he friction coefficients. The slope of the f_{app}Re vs. Re lines were shown In Fig 4, are nearly identical for each aspect ratio, and they only differ by translating to a higher f_{app}Re value as the aspect ratio decreases. This makes intuitive sense because a fluid in a channel of larger aspect ratio will have lower velocity gradients than in channels with smaller aspect ratios. From Fig 4, when the aspect ratio becomes smaller there is a smaller difference among f_{app}Re values for all Reynolds numbers considered .

International Journal of Engineering Research & Technology (IJERT)
ISSN: 2278-0181
Vol. 8 Issue 07, July-2019

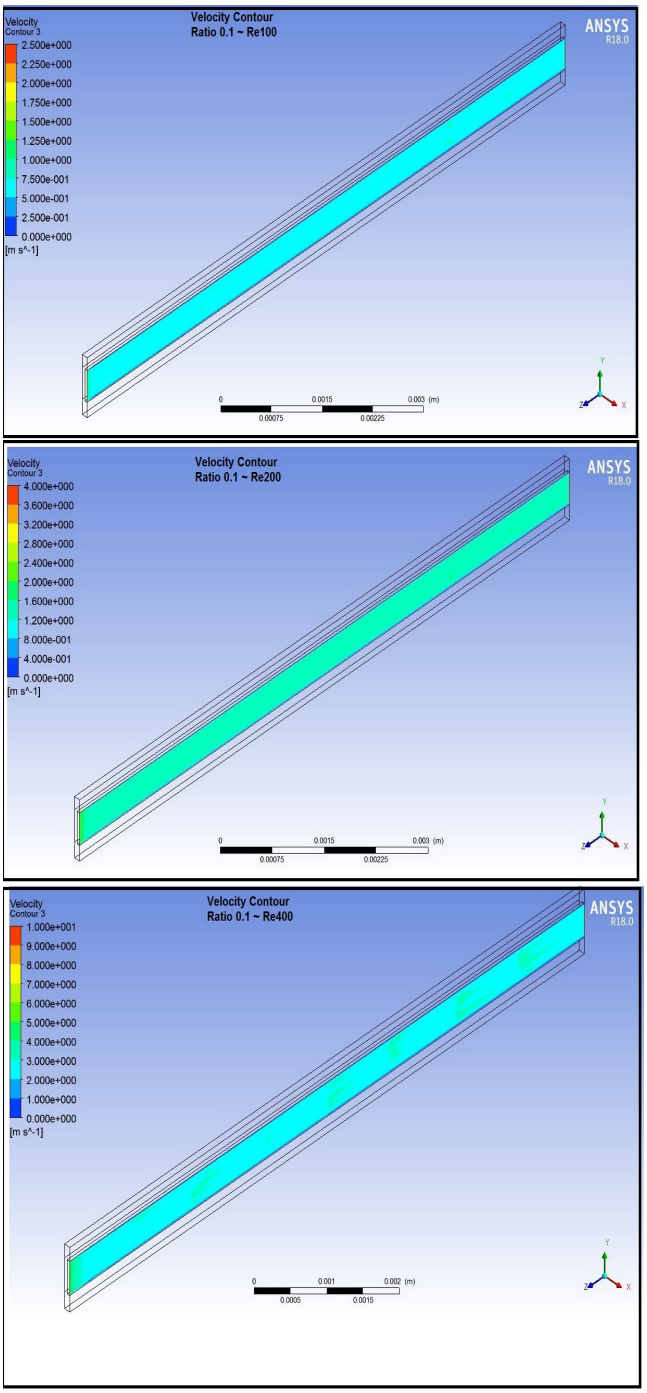

Fig. 4. Velocity Contour at 0.9 mm for aspect ratio of 0.1 with varying Reynolds Number (100, 200 and 400 respectively)

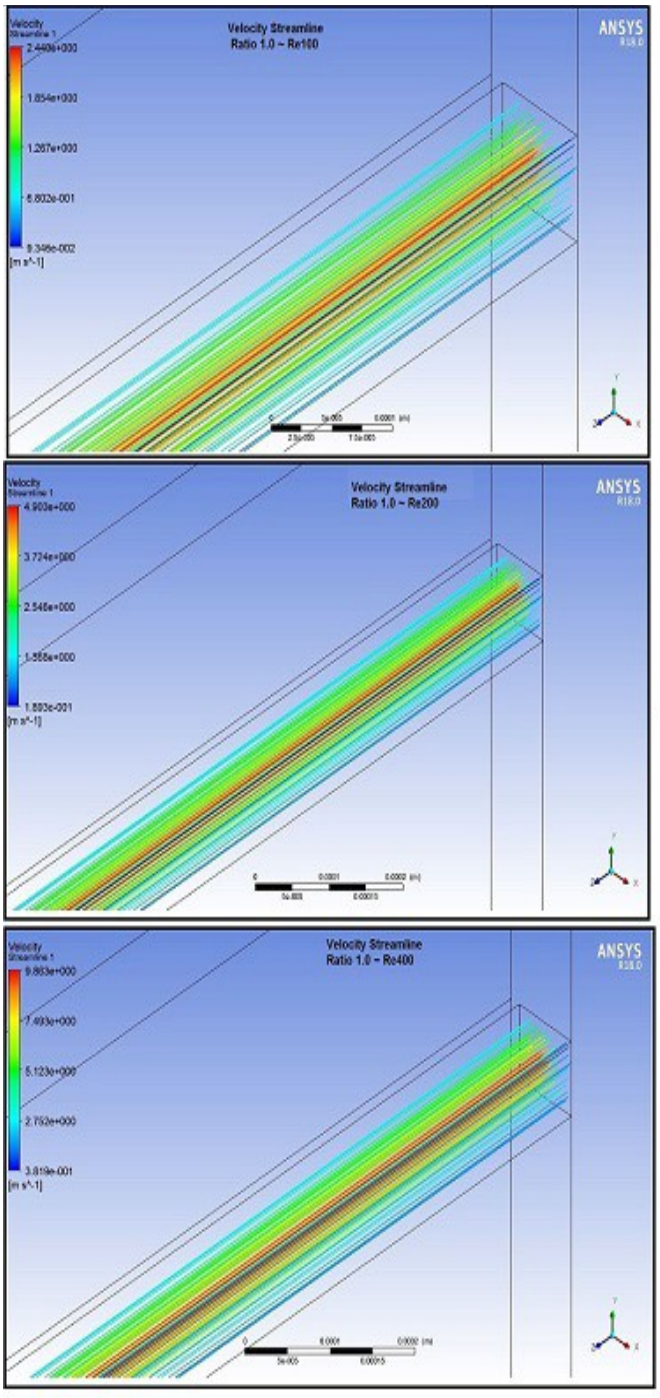

Fig. 5. Velocity Streamlines for Reynolds Number 400 and varying Aspect Ration (0.1, 0.5 and 1 respectively)

As cited in Section I, a motivation for this work is to serve as a fluid flow predictor in microchannels so for optimum performance the external systems may be designed . In most microchannel experiments,in the microchannel devices a flow loop is constructed must to provide a constant temperature fluid, which requires knowledge of the total pressure drop across the microchannel array.the microchannels are not long compared to macro-sized channels still the small hydraulic diameters cause short microchannels to have very large pressure drops for laminar flows .

Using the data from the pressure fields,The pressure drop across a single channel was determined for each geometry and flow rate. The number of channels in the array (110) were multiplied by the flow rate per channel, and the system characteristic curves were produced as shown in Fig 5. These characteristic curves could be used for selecting an appropriate pump for fiuid flows in the microchannel array. For a given flowrate,compared to all other channels, A lower pressure drop has been observed in the 0.10 aspect ratio channel . Even though all channels have the same hydraulic

International Journal of Engineering Research & Technology (IJERT)
ISSN: 2278-0181
Vol. 8 Issue 07, July-2019

diameter (Fig 4 and 5) This is an important result because of this channel has the largest apparent friction coefficient but the lowest pressure drop for a given flow rate . By using the relationship given in equation and the *fapp*Re data given in Figure 4 the pressure drop information could also be computed . The values of convective thermal resistance at both the channel inlet and outlet for all Reynolds numbers and aspect ratios considered were shown in Fig 6.For understanding the temperatures of subtrate as a function of water flow rate and channel geometry,.

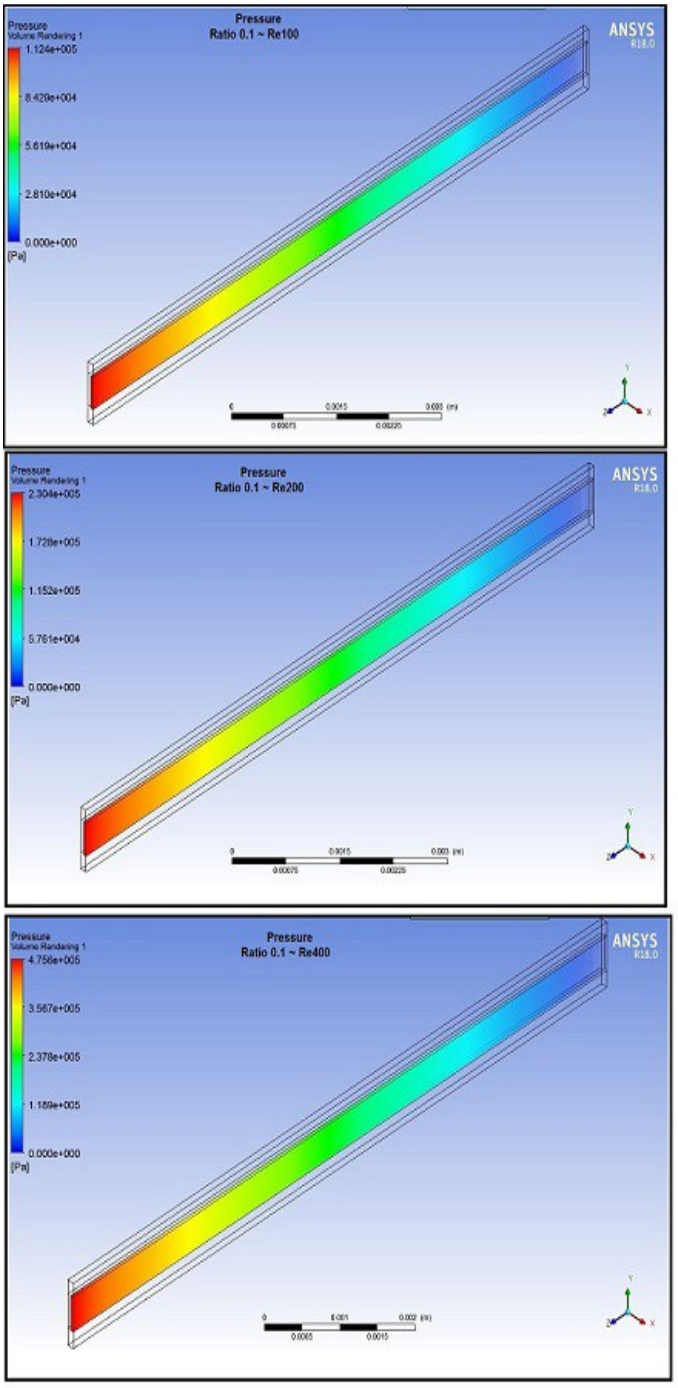

Fig. 6. Pressure Contour at 0.9 mm for aspect ratio of 0.1 with varying Reynolds Number (100, 200 and 400 respectively)

This figure serves as a useful tool Temperatures of substrate can become very high at low flow rates as evidenced by the high values of thermal resistance at high aspect ratios and low Reynolds number . In these results,thermal values for Re = 50 are not provided for aspect ratios 1.0, 0.75 and 0.50 because energy balance calculations indicated that the fluid would reach boiling temperatures. Boiling of liquid flows in microchannels has been the topic of many investigations, but in the present study it is not considered. The temperatures of substrate become very close to the liquid inlet temperatures,For high Reynolds numbers.This allows us to extrapolate that the microchannels can dissipate heat loads larger than 90 W/cm2 for Reynolds number above 400 before temperatures of substrate reach very high values

TEMPERATURE CONTOUR

The average temperature of the fluid is shown in Fig 7 as a function of channel length and Reynolds number for the aspect ratio of 0.50. For over 95% of the channel length for all Reynolds numbers considered the flow is thermally fully developed With the exception of the short thermal entry length.The average temperature of the fluid is a linear function of x for downstream of the entry length, and the mean temperature values of the fluid at the channel exit are consistent with those obtained by a system energy balance as given by Eq. (1). The mean temperature of the fluid distribution in this study for all aspect ratios can be approximated as linear between the inlet and the outlet temperature as predicted by Eq. (1).

The maximum temperatures of silicon substrate for each case of Reynolds number and aspect ratio shown in Fig 8. The important consideration is maximum substrate temperature occurs at the location of the heat source, which is the circuitry or a heater integrated location. To calculate thermal stresses and avoid high-temperature operating conditions of the system, designer must know the max temperature allowed by the system. For small aspect ratios the temperature of substrate does not vary greatly as a function of Reynolds number . Channels have high maximum substrate temperatures for low Reynolds numbers and Larger aspect ratios. Reynolds number more then 200 does not shows much effect on the maximum temperature of substrate for any particular case of aspect ratio.

In Fig 9 and Fig 10 temperature contour plots for slices within a 0.10 aspect ratio channel for a silicon substrate and a copper substrate, respectively. The thermal results are displayed for a copper substrate at the only locations of contour plots due to its very high thermal conductivity Copper was considered as an effective tool to explain the thermal energy transfer within the solid.The channel mid plane location at each of the slices through the fluid channel occurs. The thermal boundary conditions implemented on the computational domain for the Reynolds number = 100 case is shown in the Fig 9 . At the y = 900ìm boundary, The constant heat flux boundary condition results a temperature gradient . The y = 0 boundary shows zero temperature gradient indicates the thermally insulated boundary condition. Fluid temperatures along the lower y-boundary of the channel (south wall) are lower than the substrate temperature.

International Journal of Engineering Research & Technology (IJERT)
ISSN: 2278-0181
Vol. 8 Issue 07, July-2019

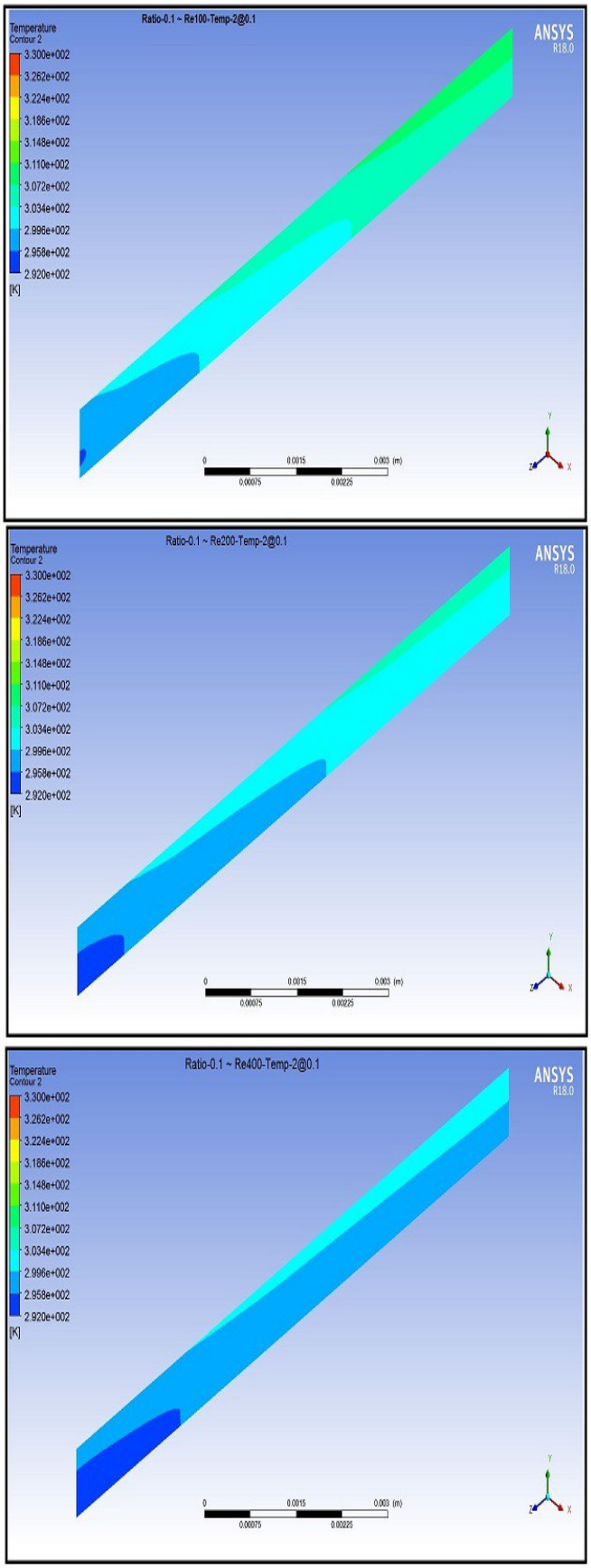

Fig. 7. Temperature Contour at 0.9 mm for aspect ratio of 0.1 with varying Reynolds Number (100, 200 and 400 respectively)

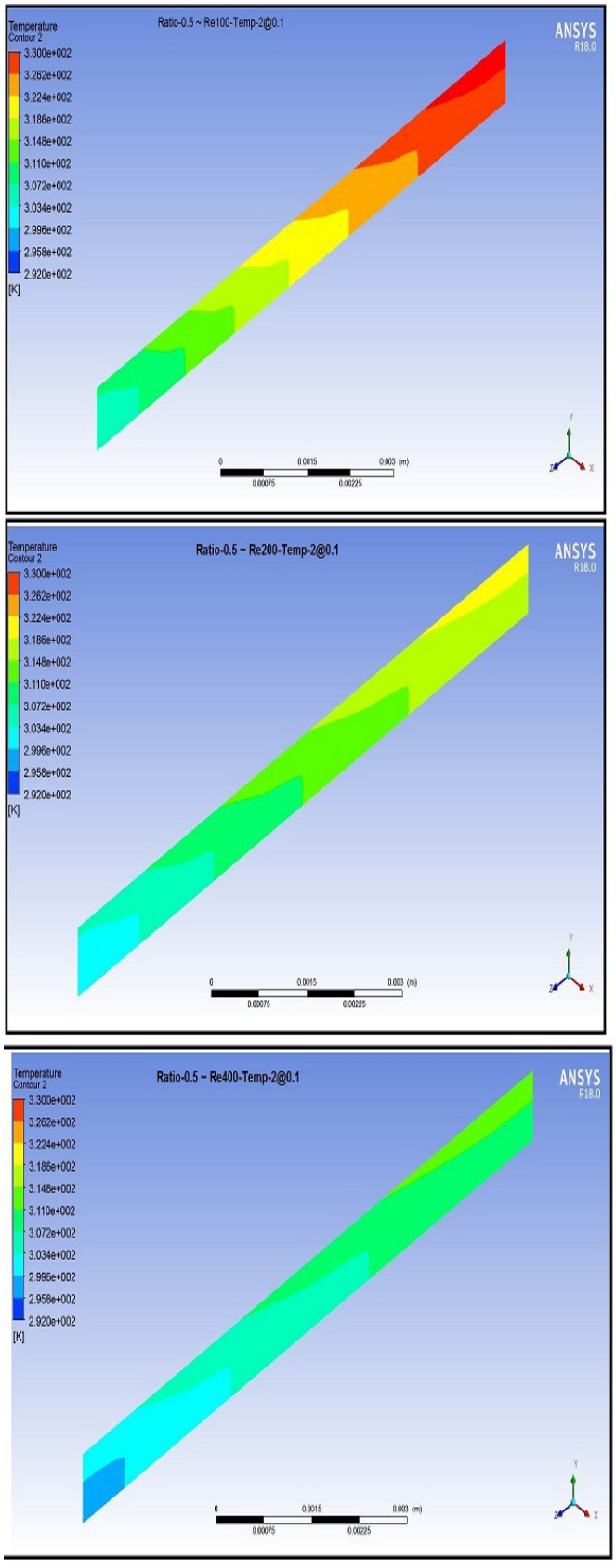

Fig. 8. Temperature Contour at 0.9 mm for aspect ratio of 0.5 with varying Reynolds Number (100, 200 and 400 respectively)

International Journal of Engineering Research & Technology (IJERT)
ISSN: 2278-0181
Vol. 8 Issue 07, July-2019

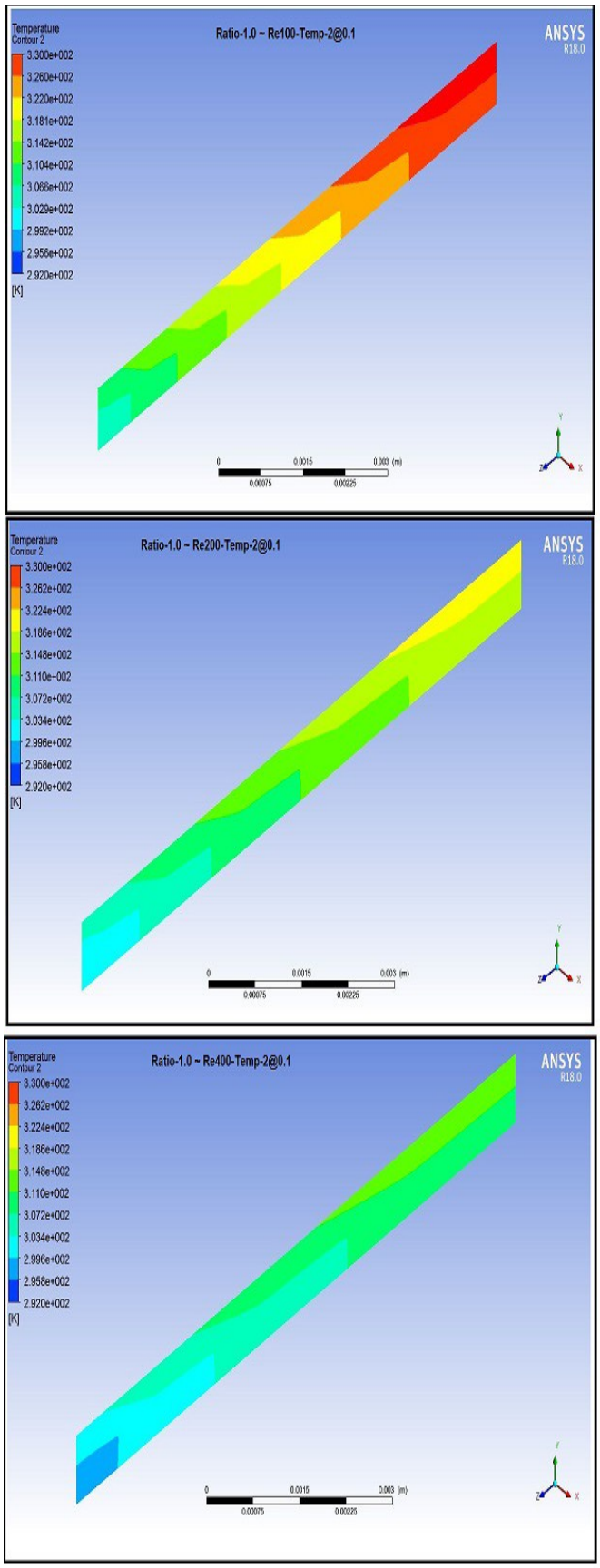

Fig. 9. Temperature Contour at 0.9 mm for aspect ratio of 1 with varying Reynolds Number (100, 200 and 400 respectively)

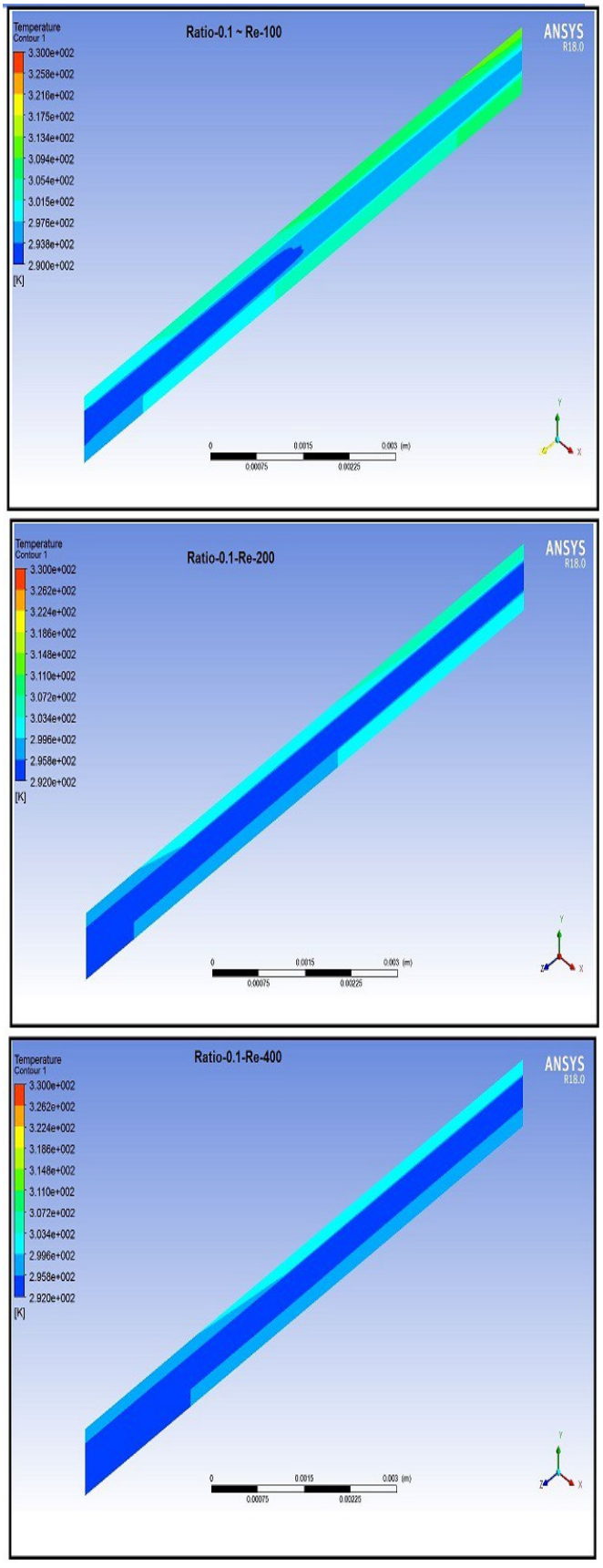

Fig. 10. Temperature Contour at 0.1 mm for aspect ratio of 0.1 with varying Reynolds Number (100, 200 and 400 respectively)

International Journal of Engineering Research & Technology (IJERT)
ISSN: 2278-0181
Vol. 8 Issue 07, July-2019

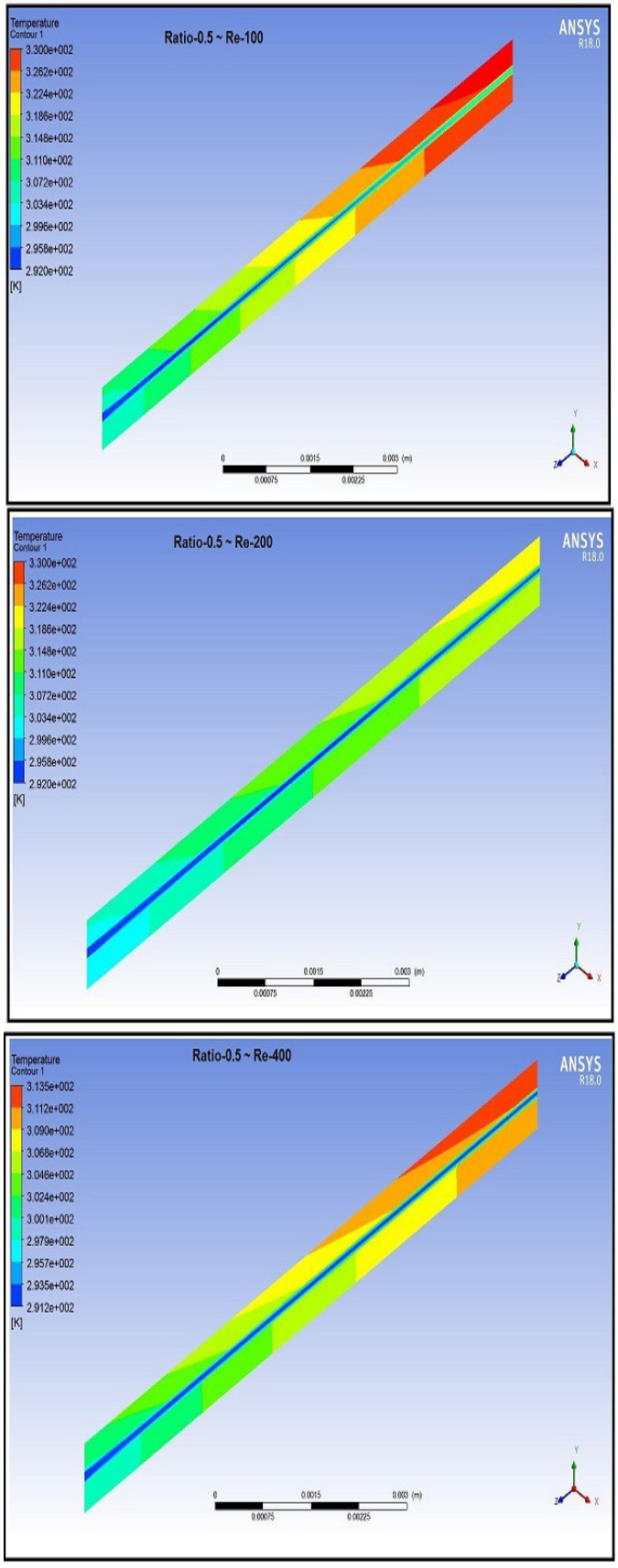

Fig. 11. Temperature Contour at 0.1 mm for aspect ratio of 0.5 with varying Reynolds Number (100, 200 and 400 respectively)

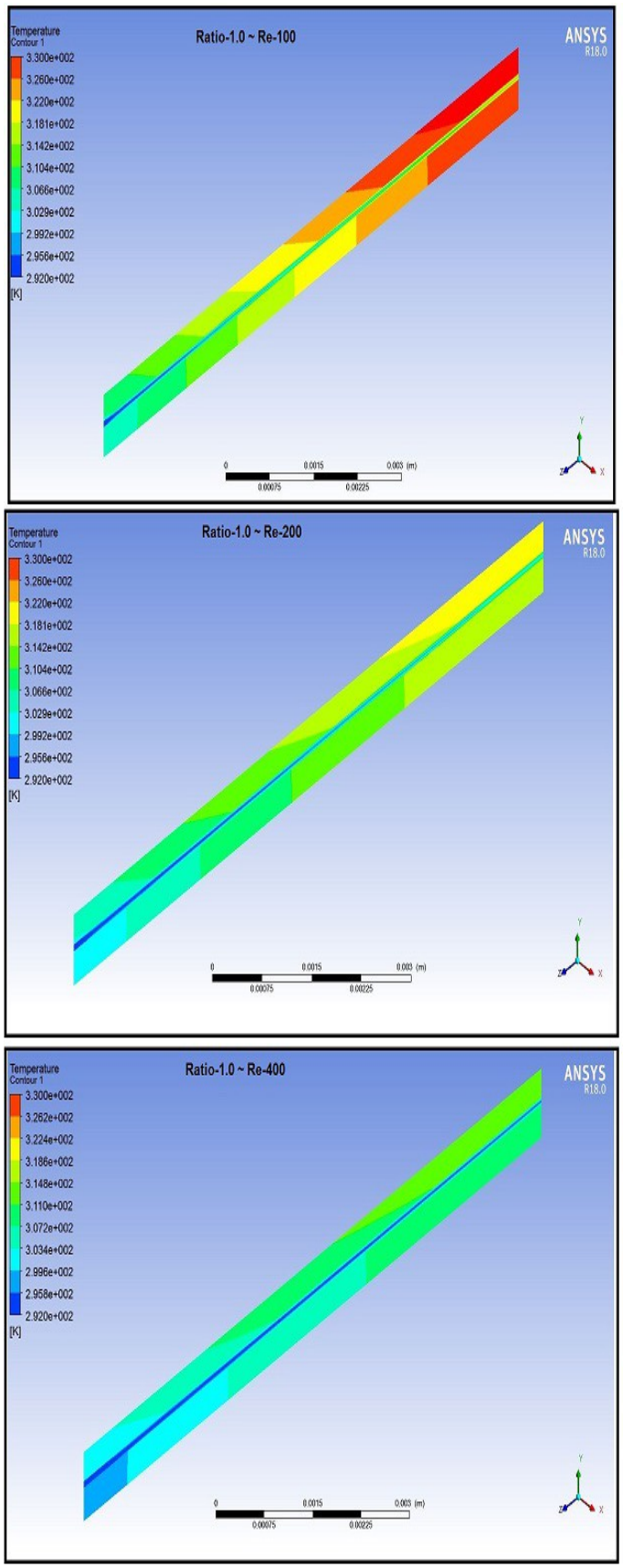

Fig. 12. Temperature Contour at 0.1 mm for aspect ratio of 1. with varying Reynolds Number (100, 200 and 400 respectively)

International Journal of Engineering Research & Technology (IJERT)
ISSN: 2278-0181
Vol. 8 Issue 07, July-2019

This indicate that the thermal energy travels all sides of the fluid channel from the heat source.Along the lower y-boundary of the channel, The temperature distributions show a large temperature gradient in the fluid. This shows that a non-trivial quantity of energy is transferred along the lower y-wall to the fluid. Fig 10 shows the temperature distributions because of the higher thermal conductivity of subtrate, there is better heat spreading .Between the silicon and copper cases The substrate and fluid temperatures seams to be the same ,but the temperature difference between the outlet and inlet of the substrate is smaller for the copper case than for the silicon case. The result of this is that the the outlet thermal resistance is decreased and inlet thermal resistance is increased gradually for the copper substrate as compared to the silicon substrate. When compared with the liquid in the copper microchannel, The temperature distribution of the liquid in silicon microchannel shows a greater temperature gradient in the y-direction . Due to this thermal energy spreads slowly in the silicon subtrate, and in the copper substrate the solid region at the south end of the channel has attained a higher temperature by the way of conduction. The amount of heat transfer from the top and bottom walls are comparable to each other. The copper substrate, that allows nearly identical temperature gradients of the fluid along with the north and south walls, which implies that the maximum substrate temperature is reduced because of the better heat spreading in the copper.

The theme of the Experiment is to analyze viscous heating effect. In this case, the mean temperature of the fluids varied by only 1.76% at the channel exit with respected to the inlet temperature The terms that include are velocity gradients, high Reynolds number flows in geometries that cause large velocity gradients will more likely exhibit viscous heating than other cases. The mean temperature of the fluid is calculated as a function of channel length for each case. Fig 11 compares the numerical results for the cases of non-viscous heating and viscous heating for the á = 0.10 case. These factors became the impetus for choosing Re = 400, á = 0.10, and á = 1.0 for the study of viscous heating. The mean temperature as a function of channel length in a channel of á = 1.0 for the non-viscous heating and viscous heating cases as shown in Fig 12. The average temperature of the fluids of the non-viscous heating and viscous heating cases differed by 0.98%. The temperature difference between outlet and inlet was considered for each case. From experiments, it is evident that viscous heating is not an important consideration for channels, but the effect of viscous heating may need to be considered for small aspect ratio or much longer channels or channels of very small hydraulic diameter. Finally, the channel with a higher aspect ratio exhibits a higher temperature rise compared to large aspect ratio.

IV. Conclusions

A numerical study was carried out which simulated 3 dimensional fluid flow and heat transfer in a repeating section of a microchannel array. Rectangular microchannels with a hydraulic diameter of 86.58ìm were studied as aspect ratios varied from 0.10 to 1.0 and Reynolds numbers ranged from 50 to 400. The difficulty arised due to conjugate nature of the heat transfer problem,the thermally boundary condition was improved. The three dimensional continuity equations and Navier-Stokes were solved using the SIMPLE algorithm, and the 3 dimensional convection-diffusion energy equations were simultaneously solved in both the solid and fluid regions after a converged velocity field was obtained,. to accurately model repeating nature of the geometry .

The following conclusions were made:

1. The continuum hypothesis holds for liquid flows in the channel sizes considered, and Navier-Stokes equations with no-slip boundary conditions also applied to model the cases considered.
2. The hydraulic entrance length increased linearly with increasing friction coefficient that was observed between Reynolds numbers 50 and 400 in this study .
3. The closeness of the thermal resistance values to the experimental data lends credibility to the numerical model because the convective nature of the problem is dependent upon velocity fields. Friction factor values and convective thermal resistance values closely matched experimental data [3] so This model is a valid model for the 0.317 aspect ratio case .
4. Hydraulic diameter was not changed between the case validated against experimental data and because the continuum assumption holds due to this it is assumed that thermohydraulic results for other aspect ratios are legitimate .
5. In this study, Viscous heating is not a considerable aspect for the cases of geometry and Reynolds number is valid aspect to consider. Only a channel with smaller cross-sectional dimensions, higher Re number flows, or much longer length would require consideration of viscous heating .
6. Heat spreading increased with Increasing the thermal conductivity of the substrate, reduces the maximum substrate temperature, and equalizes the amount of heat transferred along the northern and southern channel walls .
7. Average temperature of the fluid along the channel length may be approximated from a standard energy balance for a single repeating channel geometry .
8. Values of inlet and outlet thermal resistance decrease for aspect ratios approaching 0.10 and Friction coefficient values monotonically increase for aspect ratios approaching 0.10. The inlet and outlet thermal resistances and friction coefficient values change very little For the same hydraulic diameter for aspect ratios larger than 0.50.

References

[1] A. Bar-Cohen, Thermal Management of Air- & Liquid-Cooled Multichip Modules, IEEE Trans., Components, Hybrids, & Manufacturing Technology, vol. 10, pp. 159-175, 1987.

[2] D. B. Tuckerman & R. F. W. Pease, High-Performance Heat Sinking for VLSI, IEEE Electron Device Letters, vol. EDL-2, pp. 136-139, 1981.

[3] K. Kawano, K. Minakami, H. Iwasaki, & M. Ishizuka, Development of Micro ChannelsHeat Exchanging, Proc. ASME Heat Transfer Division:

International Journal of Engineering Research & Technology (IJERT)
ISSN: 2278-0181
Vol. 8 Issue 07, July-2019

Application of Heat Transfer in Equipment, Systems, & Education, Anaheim, California, 1998, vol. 3, pp. 173-180.

[4] Y. Yener, S. Kakac, M. Avelino, & T. Okutucu, Single-Phase Forced Convection in Microchannels: A State of the Art Review, in: S. Kakac, L. L. Vasiliev, Y. Bayazitoglu, & Y. Yener (Eds.), Microscale Heat Transfer: Fundamentals & Applications, Series II, vol. 193, Springer, Dordrecht, Netherl&s, pp. 1-24, 2004.

[5] A. Bontemps, Measurements of Single-Phase Pressure Drop & Heat Transfer Coefficient in Micro & Minichannels, in: S. Kakac, L. L. Vasiliev, Y. Bayazitoglu, & Y. Yener (Eds.), Microscale Heat Transfer: Fundamentals & Applications, Series II, vol. 193, Springer, Dordrecht, Netherl&s, pp. 25-46, 2004.

[6] S. V. Patankar, Numerical Heat Transfer & Fluid Flow, Hemisphere, New York, 1980.

[7] I. Papautsky, J. Brazzle, T. Ameel, & A. B. Frazier, Laminar Fluid Behavior in Microchannels Using Micropolar Fluid Theory, Sensors & Actuators A, vol. 73, pp. 101-108, 1999.

[8] P. Wu & W. A. Little, Measurement of Friction Factors for the Flow of Gases in Very Fine Channels Used for Microminiature Joule-Thomson Refrigerators, Cryogenics, no. 5, pp. 273-277, 1983.

[9] J. Pfahler, J. Harley, H. Bau, & J. N. Zemel, Gas & Liquid Flow in Small Channels, Proc. ASME Micromech. Sensors, Actuators, & Systems, DSC-vol. 32, pp. 49-60, 1991.

[10] S. B. Choi, R. F. Barron, & R. O. Warrington, Fluid Flow & Heat Transfer in Microtubes, Proc. ASME Micromech. Sensors, Actuators, & Systems, DSC-vol. 32, pp. 123-134, 1991. 83

[11] D. Yu, R. Warrington, R. Barron, & T. Ameel, An Experimental & Theoretical Investigation of Fluid Flow & Heat Transfer in Microtubes, Proc. 4th ASME/JSME Thermal Engineering Joint Conf., Maui, Hawaii, 1995, vol. 1, pp. 523-530.

[12] P. Wilding, J. Pfahler, H. H. Bau, J. N. Zemel, & L. J. Kricka, Manipulation & Flow of Biological Fluids in Straight Channels Micromachined in Silicon, Clin. Chem, vol. 40, pp. 43-47, 1994.

[13] G. M. Mala & D. Li, Flow Characteristics of Water in Microtubes, Int. J. Heat & Fluid Flow, vol. 20, pp. 142-148, 1999.

[14] H. Y. Wu & P. Cheng, An Experimental Study of Convective Heat Transfer in Silicon Microchannels with Different Surface Conditions, Int. J. Heat & Mass Transfer, vol. 46, pp. 2547-2556, 2003.

[15] H. Ok, H. Park, W. Carr, J. Morris, & J. Zhu, Particle-Laden Drop Impacting on Solid Surfaces, J. Dispersion Science & Technology, vol. 25, pp. 449-456, 2004.

[16] B. Agostini, B. Watel, A. Bontemps, & B. Thonon, Liquid Flow Friction Factor & Heat Transfer Coefficient in Small Channels: An Experimental Investigation, Experimental Thermal & Fluid Science, vol.28, pp. 97-103, 2004.

[17] A. Mehta & A. Helmicki, First Principles Based Approach to Modeling of Microfluidic Systems, Proc. SPIE, Microfluidic Devices & Systems, Santa Clara,California, 1998, vol. 3515, pp. 205-215.

[18] K. C. Toh, X. Y. Chen, & J. C. Chai, Numerical Computation of Fluid Flow & Heat Transfer in Microchannels, Int. J. Heat & Mass Transfer, vol. 45, pp. 5133-5141, 2002.

[19] M. N. Sabry, Scale Effects on Fluid Flow & Heat Transfer in Microchannels, IEEE Trans., Components & Packaging Technologies, vol. 23, pp. 562-567, 2000.

[20] B. Xu, K. Ooi, N. T. Wong, & W. K. Choi, Experimental Investigation of Flow Friction for Liquid Flow in Microchannels, Int. Comm. Heat Mass Transfer, vol. 27, pp. 1165-1176, 2000.

[21] A. G. Federov & R. Viskanta, Three-Dimensional Conjugate Heat Transfer in the Microchannel Heat Sink for Electronic Packaging, Int. J. Heat & Mass Transfer, vol. 43, pp. 399-415, 2000. 84